Quaternary International 219 (2010) 121–133

Contents lists available at ScienceDirect

Quaternary International

journal homepage: www.elsevier.com/locate/quaint

The Crotone series: A synthesis and new data

Jean-Pierre Suc [a,1,*], Nathalie Combourieu-Nebout [b], Guy Seret [c,2], Speranta-Maria Popescu [d], Stefan Klotz [e], François Gautier [f], Georges Clauzon [g], John Westgate [h], Donatella Insinga [i], Amanjit S. Sandhu [j,h]

[a] Laboratoire PaléoEnvironnements et PaléobioSphère (UMR 5125 CNRS), Université Lyon 1, Campus de La Doua, bâtiment Géode, 69622 Villeurbanne Cedex, France
[b] Laboratoire des Sciences du Climat et de l'Environnement (UMR 1572), Orme des Merisiers, Centre de Saclay, 91191 Gif sur Yvette Cedex, France
[c] Laboratoire de Paléontologie et Paléogéographie, Université Catholique de Louvain, 3 place L. Pasteur, 1348 Louvain la Neuve, Belgium
[d] IUEM, Domaines océaniques (UMR 6538 CNRS), 1 place Nicolas Copernic, 29280 Plouzané, France
[e] Geographical Institute, University of Tübingen, Rümelinstrasse 19-23, 72070 Tübingen, Germany
[f] 20 Mirabeau str., 75016 Paris, France
[g] C.E.R.E.G.E. (UMR 6635 CNRS), Université Paul Cézanne, 13545 Aix-en-Provence Cedex, France
[h] Department of Geology, University of Toronto, 22 Russell Street, Toronto, Ontario M5S 3B1, Canada
[i] Istituto Ambiente Marino Costiero (IAMC-CNR), calata Porto di Massa, Interno Porto di Napoli, 80133 Naples, Italy
[j] Physical Sciences Division, University of Toronto, Scarborough Campus, 1265 Military Trail, Scaborough, Ontario M1C 1A4, Canada

ARTICLE INFO

Article history:
Available online 29 January 2010

ABSTRACT

The Crotone series is undoubtedly the best-studied Early Pleistocene succession in the world. Its matchless location and sedimentary conditions contribute to optimal achievements in biostratigraphy, magnetostratigraphy, cyclostratigraphy, and finally chronology. Robust stratigraphic correlations are established between the Semaforo and Vrica areas thanks to field surveys, a cored borehole, and ash mineralogy and geochemistry. The Crotone series covers the time-interval from 2.47 to 1.21 Ma and displays 30 complete glacial–interglacial cycles, from MIS 97 to MIS 37.

Insolation cycles are recorded from i-236 to i-116 by combining lithology (sapropels) and palynology (amorphous organic matter and abundance in pollen grains of riparian trees, two indices of anoxic condition development and runoff intensity, respectively). The understanding of Early Pleistocene glacial–interglacial pollen records is clarified as the response of vegetation to the strong interaction between precession and obliquity has been analysed along several successive climatic cycles. Modern pollen records from the Rhône mouth shed light on the conditions of deposition of the sapropels, contributing to specify their intensity and duration.

1. Introduction

The Crotone series is internationally known and has been intensively studied since it was proposed as the key-locality for the Pliocene–Pleistocene boundary (Selli et al., 1977; Aguirre and Pasini, 1985). It has been chosen for containing the Global Stratotype Section and Point (GSSP) of the base of the Pleistocene placed within one of its members, the Vrica section (Cowie et al., 1986), as formally published by Pasini and Colalongo (1997). The recent decision of the International Union of Geological Sciences to lower the Pliocene–Pleistocene boundary down to 2.588 Ma, as described by Head et al. (2008), follows the previous proposals by Zagwijn (1974), Suc and Zagwijn (1983), Partridge (1997), Suc et al. (1997) and changes the Vrica GSSP which henceforth will mark the base of the Calabrian Stage. Nevertheless, during the last decades, the Crotone series has been established as a robust reference for the Mediterranean region and global climate reconstruction at the onset of the glacial–interglacial cycles of the Northern Hemisphere (Combourieu-Nebout and Vergnaud Grazzini, 1991; Combourieu-Nebout, 1993; Combourieu-Nebout et al., 2000; Klotz et al., 2006; Joannin et al., 2007) and for cyclostratigraphy (Hilgen, 1991; Lourens et al., 1996, 1998; Klotz et al., 2006; Joannin et al., 2007).

* Corresponding author. Tel.: +33 472448590; fax: +33 472431688.
E-mail addresses: jean-pierre.suc@univ-lyon1.fr, jeanpierre.suc@gmail.com (J.-P. Suc), nathalie.nebout@lsce.ipsl.fr (N. Combourieu-Nebout), guy.seret@skynet.be (G. Seret), speranta.popescu@gmail.com (S.-M. Popescu), stefan.klotz@uni-tuebingen.de (F. Klotz), clauzon@cerege.fr (G. Clauzon), westgate@geology.utoronto.ca (J. Westgate), donatella.insinga@iamc.cnr.it (D. Insinga), amanjit-sandhu@hotmail.com (A.S. Sandhu).
[1] Present address: IUEM, Domaines océaniques (UMR 6538 CNRS), 1 place Nicolas Copernic, 29280 Plouzané, France.
[2] Present address: 20 avenue Junon, 1450 Chastre, Belgium.

1040-6182/$ – see front matter © 2010 Elsevier Ltd and INQUA. All rights reserved.
doi:10.1016/j.quaint.2010.01.008

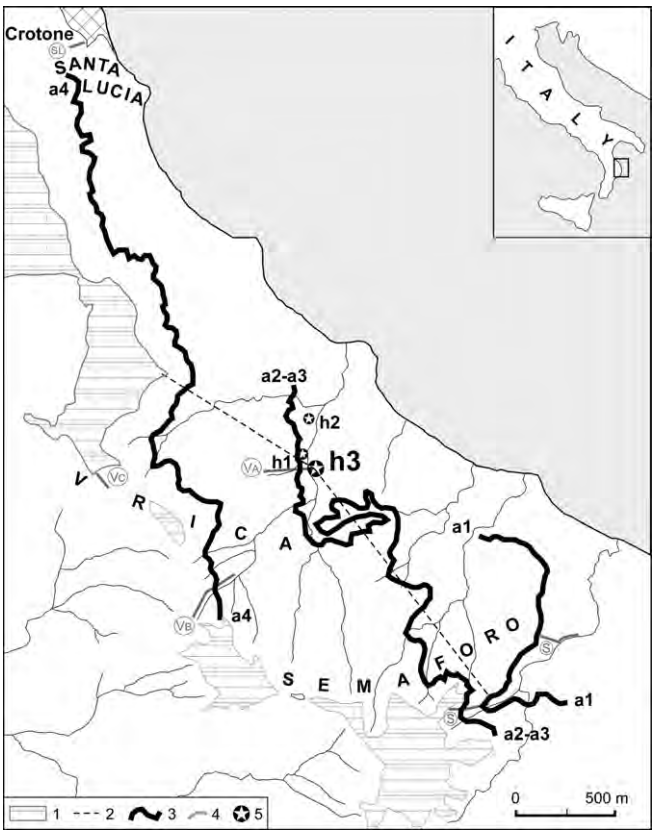

Fig. 1. Simplified geological sketch of the late Pliocene–early Pleistocene series southwards from Crotone, showing the surface trace of the ash layers (according to Selli et al., 1977); successive holes performed at the base of the Vrica section (hand-drilled holes h1 and h2: Hilgen, 1990; cored hole h3, present paper); position of the cross-section presented in Fig. 2 and detailed studied sections reported in Fig. 4. (1) Milazzian terrace; (2) cross-section; (3) ash layer; (4) studied section; (5) borehole. S, Semaforo section; VA, Vrica A section; VB, Vrica B section; VC, Vrica C section; and SL, Santa Lucia section.

The Crotone series (Fig. 1) is composed of three main sections, stratigraphically more or less overlapping, which display a continuous sedimentary record for the time-interval 2.452–1.210 Ma according to Klotz et al. (2006) and Lourens et al. (1998): the Semaforo section is entirely within the Gelasian Stage, the Vrica (A, B, C) section partly belongs to the Gelasian, partly to the Calabrian Stage, and the Santa Lucia section (= Crotone section of Zijderveld et al., 1991) belongs to the Calabrian Stage. In parallel to a reminder of the up-to-date stratigraphy–biostratigraphy–magneto-stratigraphy of the series, results (still unpublished) from the borehole cored at the bottom of the Vrica A section in 1989 are presented here. New aspects resulting from high-resolution analyses will be thus discussed as they interfere with climate reconstruction.

2. From stratigraphy to chronostratigraphy of the Crotone series

The Crotone Basin is a graben-like structure filled by post-orogenic sediments deposited since the Tortonian (Barone et al., 1982). Its northern part, the Marchesato Peninsula, uplifted and emerged during the late Lower Pleistocene (Zecchin et al., 2006), causing the sediments deposited at about 500 m bsl exposed today at 150 m asl (Fig. 2) at the foot of the Sila Massif. Southward from Crotone, the deep Pliocene–Pleistocene series (600 m thick) is gently tilted with a westwards-orientated dip of 5–15° (Selli et al., 1977). The series was truncated and somewhat protected from erosion by the more or less horizontal Milazzian marine terrace (Middle Pleistocene) (Figs. 1 and 2A). The sediments are mainly composed of grey claystones including four main ash beds and 31 brownish sapropel layers, moderately to strongly laminated (Combourieu-Nebout, 1987, 1995; Hilgen, 1991; Zijderveld et al., 1991) (Fig. 2). Some slumps have also been observed within the Semaforo and Donato sections (Combourieu-Nebout, 1987; Hilgen, 1990); they are not reported on the stratigraphic schemes of the Crotone series shown in this paper.

The relationship between the Semaforo and Vrica A sections has been clarified by Hilgen (1990) on the basis of field investigations in the intermediate sections Donato and Watertank and two hand-drilled holes (h1 and h2 on Fig. 1). However, a cored borehole remained crucial in order to obtain a continuous section and establish unequivocally the relationship between the Semaforo and Vrica A sections. Consequently, a 37.06 m length sequence (with a recovery of 84%) was performed in September 1989 using the drilling machine of C.E.R.E.G.E. (Aix en Provence, France) equipped with a Mazier core bit (length: 1 m).

2.1. Hole h3

This borehole was cored precisely at the base of the Vrica A section (Figs. 1 and 2A; Plate 1). Below 3.51 m of disturbed deposits, more or less homogenous blue–grey clays were interrupted by (Fig. 2A and B):

- a very thin (incomplete?) sapropel layer (thickness: 14 cm) at 7.05 m depth at the junction of two successive cores;
- a sapropel layer at 10.25 m depth (thickness: 1 m – recovery: 65%) interrupted in its lower half by at least 15 cm of grey clays;
- a thin ash layer (thickness: 3 cm) at 12.06 m depth.

The upper sapropel was not previously observed by Hilgen (1990) while the uppermost part of the lower sapropel was reached in hole h1. The cluster lower sapropel – ash probably correspond to that revealed in hole h2 by Hilgen (1990). They may be considered as ash 2 and sapropel 7, respectively (Fig. 2A and B). As a consequence, the upper sapropel of hole h3 should be interpreted as a fragment of sapropel 8 (Fig. 2A). It should be remembered that the Vrica A section starts at the base with an ash directly overlain by a sapropel (Figs. 2A and 5; Plate 1). Hilgen (1990) proposed this ash as equivalent to ash 3. Thus, the overlying sapropel is sapropel 9 with respect to the Semaforo stratigraphic succession (Fig. 2A). Fig. 5 illustrates some differences in thickness between holes 1, 2 and hole 3. Yet, the boreholes have not been performed at the same place (Fig. 1) and the measured depth is more precise in the cored h3 borehole than in the hand-drilled h1 and h2 boreholes. Such differences can be easily accepted as the result of the variability in thickness of the various layers of the Crotone series (Hilgen, 1990). Hilgen (1990) indicates that sapropel 7 may be duplicated as observed in hole h3 (Figs. 2B and 5). The hole h3 stratigraphy is fully consistent with the exposed uppermost Semaforo section as reported by Gautier (1990). Now, hole h3 lithology supports and somewhat precises the stratigraphic relationships between the Semaforo and Vrica sections proposed by Hilgen (1990) (Fig. 2A). Sapropels recorded in hole h3 do not present the same aspect as the exposed ones. The latter are more laminated and altered, probably because of oxidation. In addition, an in-depth field survey of sapropels and clays indicated significant differences in thickness between various exposures of the Crotone series. This explains why sapropel 6 was not recorded in hole h3.

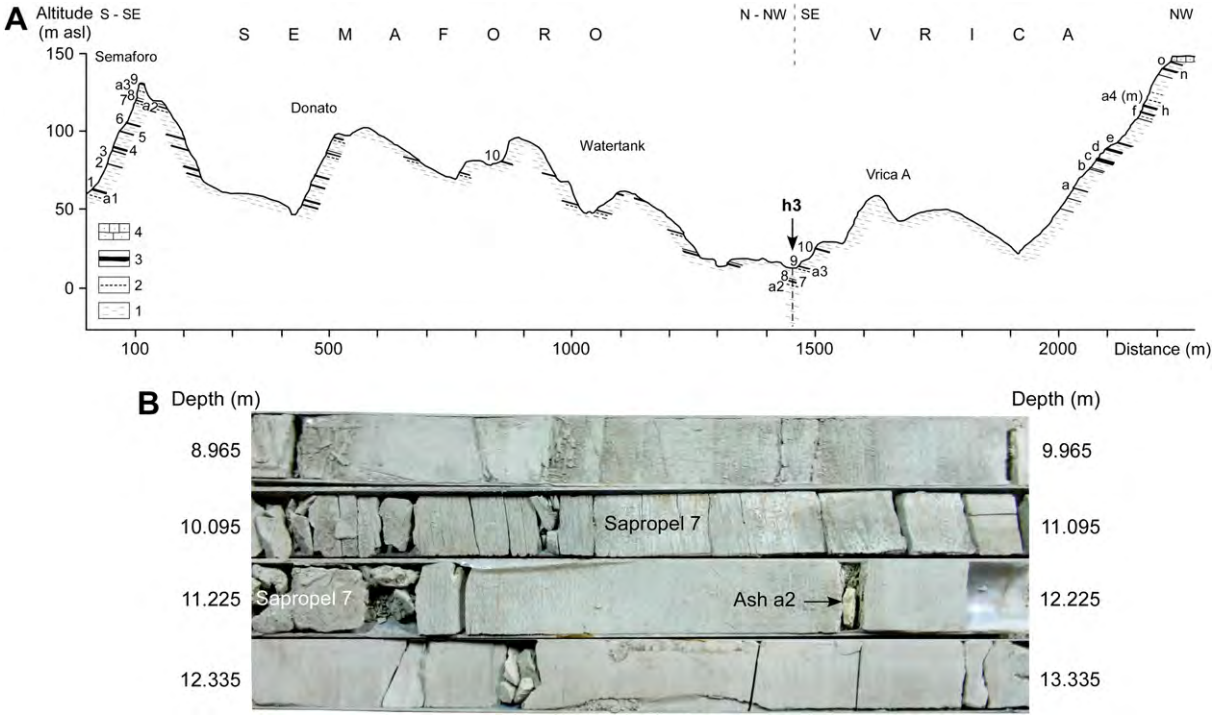

Fig. 2. Stratigraphy of the Semaforo to Vrica areas. (A) Cross-section from the lower part of the Semaforo section to the top of the series in the area of the Vrica A section, showing the intermediate sections (Donato, Watertank) by Hilgen (1990). Thickness and dip are exaggerated. (1) Clays; (2) ash; (3) sapropel; and (4) Milazzian calcarenite. Sapropels are numbered from 1 to 10 (Semaforo area) and from a to o (Vrica area), main ashes from a1 to a4 (= m: Pasini and Colalongo, 1997). (B) Some cores with respective depth of hole h3 with location of ash a2 and sapropels 7 and 8.

2.2. Ashes: a tool for stratigraphic relationships

Six volcanic ash layers have been analysed: three from the Semaforo section (ashes a1, a2 and a3), one from the hole h3 (ash a2), and two from the Vrica section (ashes a3, a4 = m) (Fig. 2). Heavy mineral associations were identified using a petrographic microscope. Fifty-four analyses of mineral phases were obtained using electron microprobe analysis at the CAMST Centre of the Université Catholique de Louvain. Fifteen average mineral compositions are calculated for the main oxides (Table 2).

Table 1 shows the summarized mineralogical comparisons of Semaforo ash a2 and ash from hole h3 Semaforo ash a3 and the ash exposed at the base of the Vrica A. Semaforo ash a1, at the lower part of the sequence, and Vrica layer m (= ash a4), at the upper part, cannot be correlated with any other layer.

The geochemical analyses back up these correlations (Table 2). Hornblende and biotite compositions are similar in Semaforo ash a2 and Vrica h3 ash as well as orthopyroxene and clinopyroxene composition that allows correlating Semaforo ash a3 with Vrica A (base) ash. These findings support Hilgen's (1990) hypothesis that the ash recorded in borehole h3 is related to ash a2 and the ash exposed at the base of the Vrica A section to ash a3 (Fig. 2A).

Pyroxenes are mostly represented by augite ($Ca_{43}Mg_{46}Fe_{11}$ to $Ca_{43}Mg_{42}Fe_{15}$, Mg# from 74 to 80) and enstatite ($Ca_3Mg_{73}Fe_{24}$ to $Ca_2Mg_{62}Fe_{36}$, Mg# from 63 to 75), and one sample of subcalcic augite ($Ca_{29}Mg_{49}Fe_{22}$), according to the Morimoto and subcommittee members (1988) classification (Fig. 3A). In ash layer a3, at the base of the Vrica section, a likely metamorphic clinopyroxene (diopside, $Ca_{45}Mg_{51}Fe_4$, with Mg# = 92) was also found. Amphiboles are represented by Mg hornblende found in both layers a1 and a2, Fe–Mg and Ti–Mg–hastingsitic hornblende found in layer a2, according to the Leake et al. (1997) classification. Biotite from layer a2 has relatively high Ti content (4.5 wt.% TiO_2). Zoning in the analysed phases has not been observed. The presence of orthopyroxene, clinopyroxene, amphibole and biotite as mafic minerals strongly suggests a mafic-intermediate composition of the source rock with a calc-alkaline affinity (arc-type).

A change in the pyroxene composition took place from the bottom to the top of the succession: orthopyroxene: ($Ca_2Mg_{62}Fe_{36}$) (a1) to ($Ca_3Mg_{73}Fe_{24}$) (a3).

The composition of minerals in the Vrica and Semaforo ashes suggests that different magma compositions reached this area. An association of two different augites in ash a4, of an augite and a diopside in Vrica ash a3, of two different amphiboles in Vrica h3 ash a2 also indicates different magmatic origins of the same volcanic ash layer. Chemical analyses of pyroxenes reveal a calc-alkaline affinity for all the samples as also shown by the Ti–Al diagram (Fig. 3B; Letterier et al., 1982).

Subduction-related volcanism of calc-alkaline affinity took place during the evolution of the southern Tyrrhenian Basin (Argani and Savelli, 1999). The older products crop out in Sardinia and are related to the Oligo-Miocene (32–13 Ma) volcanism while the younger products (1–0 Ma) are sourced from the Aeolian Islands vents. During an intermediate phase of this time-space evolution, volcanic centres of Pliocene age (5–2 Ma) were arranged along an arcuate structure (Central Tyrrhenian arc; Argani and Savelli, 1999) running from the Anchise seamount (5.2–3.6 Ma; Savelli, 1988) in the south to Ponza Island in the north (4.2–1 Ma; Cadoux et al., 2005). Mafic to intermediate rocks with calc-alkaline affinity have been found along this arc and they include the basalts and andesites recovered in deep boreholes from the Volturno River plain along the southern Campania coast (2 ± 0.4 Ma: K/Ar age; Barbieri et al., 1979; Di Girolamo et al., 1997) and some lavas in the Marsili basin (3–1.7 Ma; Beccaluva et al., 1990; Peccerillo, 2005 and references therein). Compositions of pyroxenes from the Campania deposits are reported in detail in Fig. 3; the data closely match the

Plate 1. (1). General view of the Semaforo section showing sapropels 1 to 6 and ash a1. (2) Detailed view of ash a1 (Semaforo section). (3) Coring hole h3 in front of the exposed ash a3 and sapropel 9. (4) Vrica A section showing the location of the coring hole h3 and sapropels 13–15. (5) View of the Vrica B section showing sapropels 15–20. (6) Detailed view of ash a4 (Vrica B section). (7) View of the Vrica C section showing sapropels 23, 26 and 27. (8) View of the Santa Lucia section showing sapropel 30.

studied samples from the Crotone series. According to these considerations along with the proposed age of ca. 2.3 Ma for ash layer a1 (see later), a correlation of the Crotone ash layers with the southern Tyrrhenian volcanism could be proposed. The recovery of these products in the Crotone series strongly supports previous studies dealing with ash deposits in Pliocene sequences from southern Apennines and Calabria (Spadea, 1986; Guerrera and Veneri, 1989; Prosser et al., 2008) thus aiming to give further details on the eruptive history of the southern Tyrrhenian domain in Pliocene–Pleistocene times.

2.3. Stratigraphy and biostratigraphy

The stratigraphic correlations between the sections of the Crotone series is now definitely clarified as the numerous detailed field investigations from the various teams have now almost certainly recorded the complete Crotone archive (Fig. 4A; Semaforo: Combourieu-Nebout, 1995; Vrica A–Vrica B–Vrica C: Pasini and Colalongo, 1997; Santa Lucia: Zijderveld et al., 1991; hole h3: present paper). Thus, the Crotone sequence sapropel layers have been here newly re-numbered from 1 to 31 (upwards from the

Table 1
Mineralogy (in percentage) of the ash beds from the Crotone series.

Ash bed	a1	a2		a3		a4
Minerals	Semaforo	Semaforo	Hole h3	Semaforo	Vrica A (base)	Vrica (m)
Clinopyroxenes	8	2	2	36	38	38
Hyperstenes	26	1	0	51	45	9
Basaltic hornblendes	60	93	87	0.5	0	0
Others	6	3	7	12	17	53

base), the main ashes have only been numbered (a1–a4), and the minor sand beds are not reported (Fig. 4A).

The biostratigraphy of foraminifers (Fig. 4B) and nannofossils (Fig. 4C) looks rather heterogeneous. In fact, foraminifer records have been built by several scientists on various time-resolution sampling and more often on different stratigraphic intervals (Colalongo: in Selli et al., 1977; Colalongo et al., 1981; D'Onofrio, 1981; Spaak, 1983; J. Cravatte, personal information; Hilgen, 1990; F. Quillévéré: in Joannin et al., 2007)

Thus some taxonomic divergences between specialists resulted in discrepancies in the species biostratigraphic range, as observed for *Neogloboquadrina atlantica*. For these reasons, only synthetic results are presented in Fig. 4B taking into account the above-mentioned authors. Following the initial low-resolution nannofossil studies (Nakagawa et al., 1981; Cati and Borsetti, 1981), Rio et al. (1997) published a quite detailed record of the Vrica section, completed by Lourens et al. (1998) by the results from the Santa Lucia section. No nannofossil study was performed on the Semaforo section. The main biostratigraphical foraminifer and nannofossil markers are presented in Fig. 4B and C. They provide a rough calibration in order to build the age-model of the series. However, some inconsistencies persist, such as the record of *Gloconella* (*Globorotalia*) *inflata* between sapropels 8 and 9 by J. Cravatte (Combourieu-Nebout, 1987, 1990) and Hilgen (1990) that implies to predate the First Appearance Datum of this species in the Mediterranean dated at 2.09 Ma by Lourens et al. (2004). Other microfossils (ostracods and diatoms) and macrofossils (molluscs, fishes) unfortunately provide poor biostratigraphic resolution and then have not been considered in this synthesis (for details, see: Pasini and Colalongo, 1997).

2.4. Magnetostratigraphy

The magnetostratigraphy of the Vrica section (Tauxe et al., 1983) was completed later by Combourieu-Nebout et al. (1990) and Zijderveld et al. (1991) for what concerns the base of the Olduvai Event (C2n Chron) with larger amount of measurements, resulting in the stratigraphic location shown in Fig. 4D. According to Tauxe et al. (1983), the Olduvai Event (discontinuously recorded) would end at the top of sapropel d (16), while it could end 8 m above sapropel e (17) according to Zijderveld et al. (1991), i.e. the alternative is reported in Fig. 4D. Nakagawa et al. (1997) obtained a moderately divergent location of the Olduvai Event that suffers from a lack in samples at its borders (cf. for comparison: Pasini and Colalongo, 1997). Tauxe et al. (1983) pointed out another normal event almost corresponding to sapropels q (25) to s (27) that was not confirmed by Zijderveld et al. (1991). In addition, Tauxe et al. (1983) also obtained continuously reverse measurements in the Semaforo section, starting about 30 m below the base of the section in Fig. 4A and ending ca. 5 m above sapropel 6.

A palaeomagnetic study of sediments cored at hole h3 was performed in 1994 at the Geosciences Institute of Montpellier using

Table 2
Microprobe analyses of mineral phases from the studied ash layers. Mg# = molar 100Mg/Mg + Fe; Ca, Mg and Fe in mol%.

Ash bed	a1	a2			a3		a4	
Site	Semaforo	Semaforo	Hole h3		Semaforo	Vrica A (base)	Vrica (m)	
Classification	Enstatite	A(Mg hornblende)	A(Fe–Mg hornblende)	A(Ti–Mg–hastingsitic hornblende)	Enstatite	Enstatite	Augite	Augite
SiO_2	51.57	45.01	45.25	42.38	52.34	52.59	50.26	50.94
TiO_2	0.14	1.72	1.55	2.58	0.21	0.17	0.73	0.49
Al_2O_3	0.56	8.04	7.38	10.55	1.14	0.92	3.21	2.83
Cr_2O_3	0.02	0.01	0.00	0.02	0.02	0.00	0.11	0.13
FeO	22.11	13.56	14.89	10.84	18.47	13.85	9.15	6.87
MnO	0.99	0.44	0.56	0.14	0.73	0.80	0.23	0.18
MgO	22.03	14.16	13.14	14.83	24.51	24.97	15.89	16.27
CaO	1.08	11.94	11.45	11.58	1.42	1.18	19.58	21.20
Na_2O	0.02	1.54	1.40	2.15	0.00	0.01	0.31	0.21
K_2O	0.00	0.77	0.79	0.89	0.00	0.01	0.01	0.00
Mg#	0.63				0.69	0.75	0.75	0.80
Ca	2.20				2.80	2.50	40.00	43.00
Fe	36.20				29.70	24.20	14.90	11.20
Mg	61.60				67.50	73.30	45.10	45.90
Classification	Mg hornblende	Biotite	Biotite		Augite	Augite	Augite	Augite
SiO_2	43.82	36.27	35.62		50.21	51.14	53.01	52.15
TiO_2	2.06	4.59	4.58		0.51	0.41	0.11	0.15
Al_2O_3	8.08	13.77	13.57		2.76	1.95	1.50	3.55
Cr_2O_3	0.03	0.02	0.03		0.04	0.00	0.52	0.00
FeO	12.95	15.19	14.81		8.88	9.06	2.68	12.23
MnO	0.32	0.16	0.17		0.22	0.40	0.08	0.20
MgO	13.91	14.62	14.41		15.83	15.11	18.41	15.56
CaO	11.57	0.00	0.00		20.59	21.06	22.81	12.64
Na_2O	1.57	0.58	0.53		0.25	0.29	0.17	0.31
K_2O	0.90	9.08	8.76		0.01	0.01	0.01	0.14
Mg#					0.76	0.74	0.92	0.69
Ca					41.40	42.60	45.10	28.70
Fe					14.30	14.90	4.30	22.10
Mg					44.30	42.50	50.60	49.20

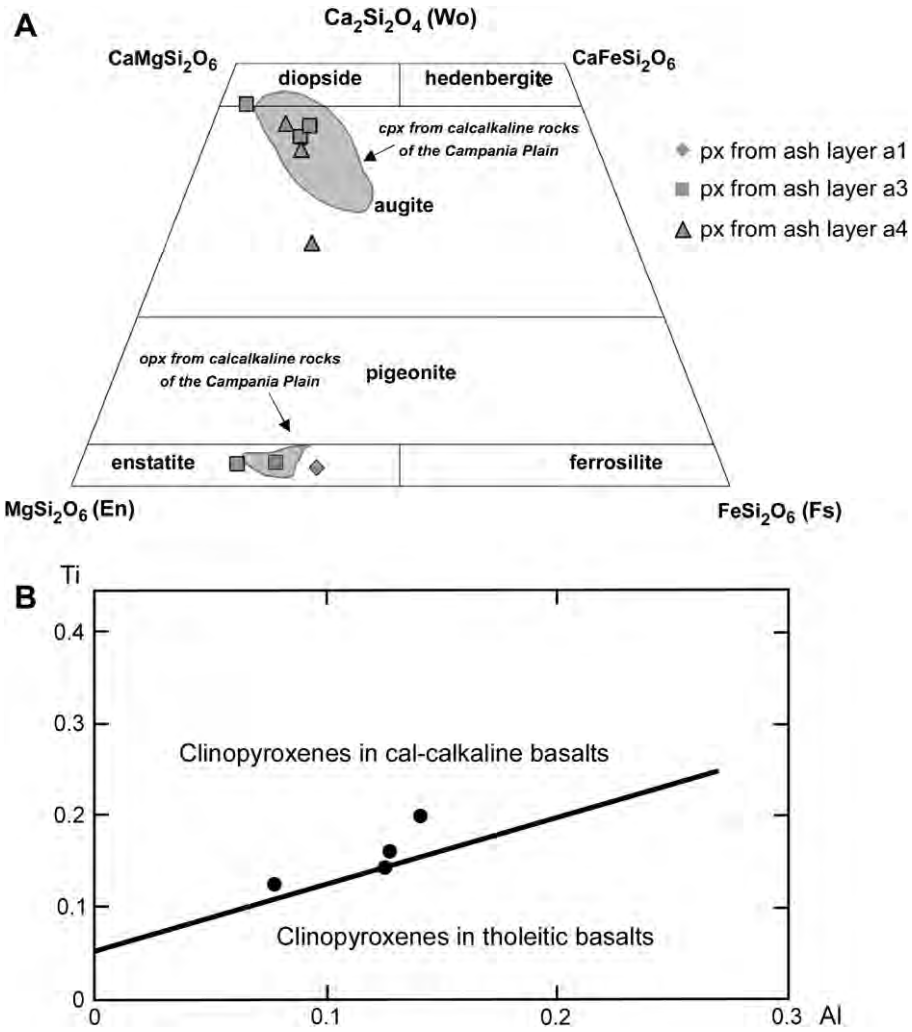

Fig. 3. Origin of rock discrimination from geochemical analyses of the Crotone ash beds. (A) Classification of the pyroxenes representative of some ash layers recovered in the Crotone series according to Morimoto and subcommittee members (1988). Composition of orto- and clinopyroxenes from calc-alkaline rocks of the Campania Plain are also shown for comparison (data from Di Girolamo et al., 1997 and from L. Franciosi, pers. comm.). (B) From Ti–Al ration discrimination for clinopyroxenes between calc-alkaline and tholeritic basalts (Letterier et al., 1982).

a TCF cryogenic magnetometer. Seventeen samples were progressively thermally demagnetised and the natural remanent magnetisation was found between 600–700 °C in temperature. Inclination was measured on samples from hole h3: a truncated normal episode was found (Fig. 5) that is here referred to the Réunion Event (C2r.1n Chron) (Fig. 4D).

2.5. Cyclostratigraphy from oxygen isotope, palynology and sapropel succession

A first relatively weak $\delta^{18}O$ record was performed both on *Uvigerina peregrina* and *Globigerina bulloides* from the Semaforo and Vrica sections (Combourieu-Nebout and Vergnaud Grazzini, 1991) (Fig. 4E). This allows several correlations with Marine Isotope Stages (MIS) (Fig. 4G). However, this preliminary study was somewhat consistent with that realised at higher resolution on *Globigerinoides ruber* from the upper Vrica B, Vrica C and Santa Lucia sections (Lourens et al., 1996) (Fig. 4E). Recently, new high-resolution $\delta^{18}O$ measurements agree and complete the Santa Lucia section one using *Globigerina bulloides* (Joannin et al., 2007) (Fig. 4E) and result in improving correlations with MIS (Fig. 4G). Sea-surface temperature has then been reconstructed using foraminifers from the upper part of the series (from sapropel 17 to the top) and appears consistent with the corresponding $\delta^{18}O$ record (Lourens et al., 1996).

The Semaforo high-resolution pollen sequence refines the correlations with vegetation glacials and interglacials respectively, i.e. with the MIS (Combourieu-Nebout, 1993, 1995) and thus a similar high-resolution (a sample/40 cm) has been extended to the Vrica A section (Fig. 4F and I). The pollen ratio between the 'thermophilous' elements (subtropical trees: Taxodiaceae, Sapotaceae, *Nyssa*, Arecaceae, etc.; plus warm-temperate trees: *Quercus*, *Carya*, *Pterocarya*, *Carpinus*, *Acer*, etc.) and the 'steppe' elements (*Artemisia*, *Ephedra*), i.e. the so-called 'Pollen Temperature Index', is considered as regional temperature change indicator (Fig. 4F). This ratio has been constructed for the Santa Lucia section, using the data from Joannin et al. (2007) (Fig. 4F).

Combining oxygen isotope curves and the Pollen Temperature Index already mentioned, it is possible to identify each glacial and interglacial, shown in Fig. 4 by white and grey bands, respectively. However, some discrepancies sometimes occur between the oxygen isotope curve and the Pollen Temperature Index such as (1) in MIS 58 and 48 (Fig. 4E and F) with high values of $\delta^{18}O$ (i.e. glacial values) recorded simultaneously with high frequencies in thermophilous plants (i.e. displaying an interglacial signal) and (2) in an opposite way MIS 57, 61 and 63 (interglacial signal in the $\delta^{18}O$ record, glacial

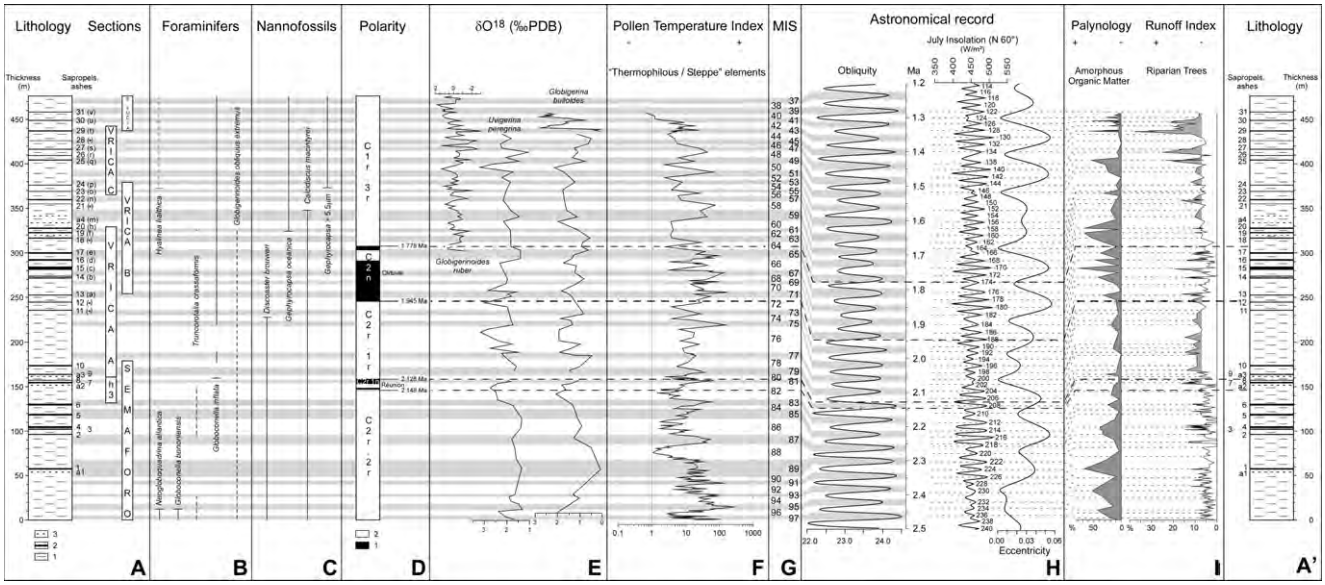

Fig. 4. From stratigraphy to high-resolution cyclostratigraphy of the Crotone series. (A) Lithology and successive studied sections reported in Fig. 1. Sapropels are numbered from 1 to 31 (with indication of their name in previous papers), main ashes are indicated (a1–a4). (1) Clays; (2) sapropel; and (3) ash. (A′) Repeated lithology and sapropel numbering only. (B) Summary of the biostratigraphy based on the main foraminifer markers (using the results from: Spaak, 1983; Hilgen, 1990, 1991; Combourieu-Nebout and Vergnaud Grazzini, 1991; Pasini and Colalongo, 1997; Joannin et al., 2007). (C) Summary of the biostratigraphy based on the main nannofossil markers (using the results from: Rio et al., 1997; Lourens et al., 1998). (D) Magnetostratigraphy (using the results from: Tauxe et al., 1983; Zijderveld et al., 1991; and Gautier, this paper). The polarity results from hole h3 are shown in Fig. 5. (1) Normal; and (2) reverse. (E) Oxygen isotope records: on *Globigerinoides ruber* (Lourens et al., 1996), *Uvigerina peregrina* and *Globigerina bulloides* from the Semaforo and Vrica sections (Combourieu-Nebout and Vergnaud Grazzini, 1991), *Globigerina bulloides* from the Santa Lucia section (Joannin et al., 2007). (F) The Pollen Temperature Index expressed by the pollen ratio 'thermophilous/steppe' elements. The data are from Combourieu-Nebout (1987) for the Semaforo and Vrica sections, from Joannin et al. (2007) for the Santa Lucia section, and new data from N. Combourieu-Nebout. The curves are plotted on a semi-logarithmic scale. (G) Relationships with Marine Isotope Stages (MIS) as discussed by Combourieu-Nebout and Vergnaud Grazzini (1991), Lourens et al. (1996) and Joannin et al. (2007) (oxygen isotope records), by Klotz et al. (2006), completed in this study (see: Pollen Temperature Index in F). Interglacials are underlined by grey bands, glacials by white bands. (H) Astronomical parameters for the time-interval 2.5–1.2 Ma (LA04 solution: Laskar et al., 2004): obliquity, July insolation at 60°N (maxima are numbered), eccentricity. Relationships between MIS and glacials–interglacials identified in the Crotone series using obliquity. (I) Palynology Runoff Index: amount of amorphous organic matter within palynological residue (Combourieu-Nebout, 1990) and frequency of riparian trees (*Platanus*, *Parrotia persica*, *Liquidambar*, *Pterocarya*, *Carya*, *Fraxinus*, *Salix*, *Populus*, *Alnus*, *Ulmus*, and *Zelkova*) in pollen records (Combourieu-Nebout, 1990, 1995; Joannin et al., 2007). The maxima considered are shaded (>7%). These proxies and the sapropels of the series are correlated to July insolation within the chronological framework previously defined using the MIS and obliquity correlation. This index corresponds to the Mediterranean Precession Related Sapropels Code (Hilgen, 1991; Lourens et al., 1998).

signal in the Pollen Temperature Index; Fig. 4E and F). Such discrepancies may be considered as the result of the rather low resolution of pollen record in contrast to the $\delta^{18}O$ record. Therefore, the oxygen isotope record is here surely considered as the most reliable record for glacial and interglacial illustration, especially when the chronological resolution of pollen record is relatively low (i.e. for the interval MIS 64–44: Vrica B and C sections *p.p.*).

Relationships with obliquity is proposed for the entire Crotone series (Fig. 4H) in comparison to those from the Semaforo (Klotz et al., 2006), Vrica B (*p.p.*), C and Santa Lucia sections (Lourens et al., 1996), and the Santa Lucia *p.p.* section (Joannin et al., 2007).

In more detail, Hilgen (1991) and Lourens et al. (1996, 1998) established a cyclostratigraphy of the Mediterranean sapropels (MPRS Code: Mediterranean Precession Related Sapropel Code) in relation to the respective precession-eccentricity influence resulting in a very accurate correlation between the Crotone sapropels and insolation cycles (as numbered in Fig. 4H and A′). Sapropels arising from intense anoxia coupled with increasing runoff are deposited during periods of precession minima (i.e. maxima of July insolation), and are therefore particularly well-expressed during eccentricity maxima (Hilgen, 1991). The sapropels represent here the observable field evidence of such orbital cycles. Today, the listing of the Crotone sapropels is considered as complete, despite the remaining questioning about the presence of a sapropel 20 m below sapropel 1, as indicated by Tauxe et al. (1983) but never found by anyone else. According to Lourens (1994), the series would run from insolation maxima 236 to 116. Hence, 30 precession related minima (i.e. July insolation maxima) are missing in the Crotone series, and more particularly 20 are missing between sapropels 1 (i-222 in the MPRS Code) and 31 (i-122 in the MPRS Code) (Fig. 4H). It has been demonstrated that the abundance of amorphous organic matter (AOM) within palynological residues (i.e. the palynofacies) reveals peaks of anoxia whether they resulted in sapropel deposition or not (Combourieu-Nebout, 1990; Suc et al., 1991; Joannin et al., 2007). This approach is helpful to illustrate the correlations with insolation maxima outside the sapropel layers (Fig. 4I), and it is successfully supported by the 'riparian trees' frequency record. The 'riparian trees' pollen grain amounts in marine coastal sediments are directly forced by river input (Beaudouin et al., 2005). This pollen index expresses the regional river input changes, i.e. discharges, and provides further direct information on the development of anoxic conditions in bottom waters in relation with runoff increase. The recent high-resolution pollen analyses, performed at a higher resolution than the palynofacies one, and the 'riparian tree pollen' curve now allow finer correlations with the insolation maxima (Fig. 4I). The 'riparian tree pollen' maxima are significantly higher in the topmost part of the series (uppermost 40 m of the Vrica C section and Santa Lucia; Fig. 4I). This probably results from increased proximity of land and river pollen source at the end of the Crotone series deposition when uplift caused the locality shallowing. Considering the information of 31 sapropels, 47 maxima in riparian trees (>6% for most; Fig. 4I) and 27 maxima in amorphous organic matter (Fig. 4I), correlations are proposed with 54 of the 57 insolation maxima between i-236 and i-122 (only i-154, i-150, and i-148 cannot be correlated; Fig. 4I). The peak in riparian trees recorded 20 m below sapropel 1, and

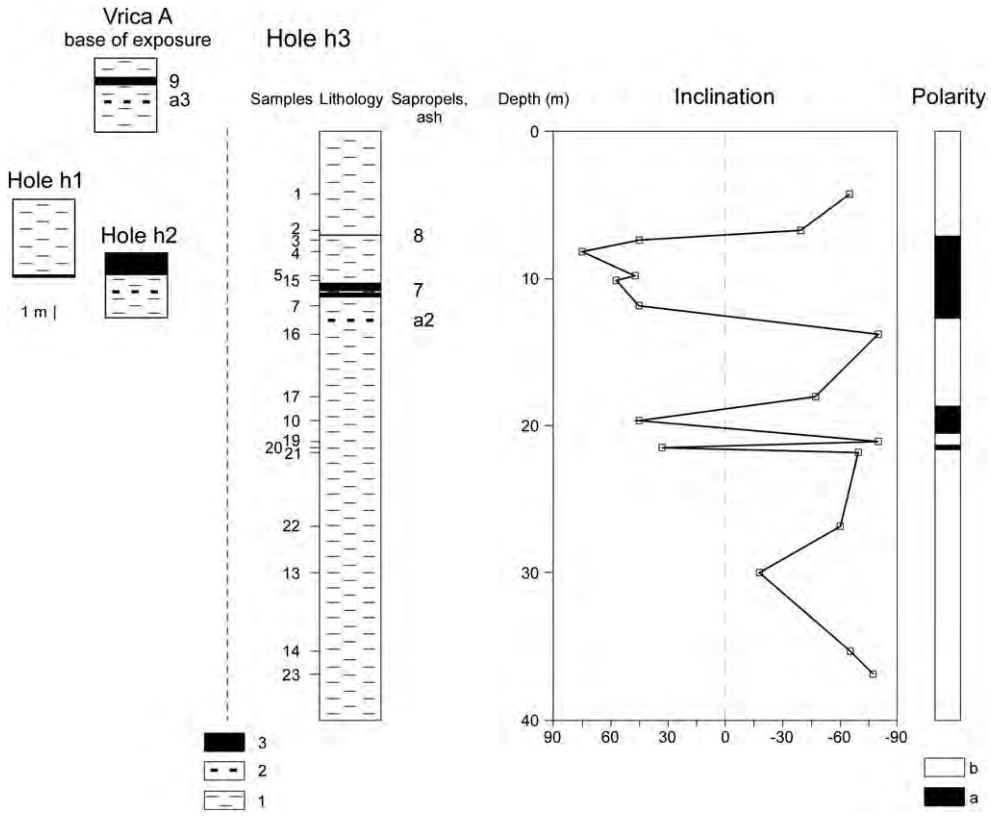

Fig. 5. Lithostratigraphy and magnetostratigraphy of hole h3. Lithostratigraphic relationship is shown with the exposed base of the Vrica section and boreholes h1 and h2 (Hilgen, 1990). (1) Grey clays; (2) ash; and (3) sapropel. (a) Normal; and (b) reverse.

correlated with the July insolation maximum i-226, may then correspond to the sapropel indicated by Tauxe et al. (1983).

Finally, combined high-resolution record of all data (biostratigraphy, magnetostratigraphy, cyclic records) results in a very accurate age-model of the Crotone series (see Fig. 4H). The alkenone method also appears to be a promising tool for high-resolution cyclostratigraphy (Cleaveland and Herbert, 2009). The age of the base of the series studied is pointed at 2.47 Ma. On the basis of these correlations, the sedimentation rate has been rather constant: about 0.45 mm/yr on average for the lower 300 m, decreasing at 0.29 mm/yr on average for the upper 175 m of the series (Fig. 6). The apparent sedimentation rate decrease is probably caused by the early Pleistocene increasing uplift of the marginal Crotone Basin which led to its shallowing and emersion. The clayey particles were more transported far off into the Ionian Basin according to the reducing local accommodation, the environment context of which evolved from slope to shelf conditions (Zecchin et al., 2006).

No concerted internationally driven action was ever established in order to investigate the Crotone series for collective sampling. Such an approach would have probably avoided data discrepancies, especially in thickness measurements. As an example, such an action by N. Ciaranfi obviously enhanced the study reliability undertaken on the Montalbano Jonico section (Ciaranfi and D'Alessandro, 2005).

2.6. Checking the age of ashes

Two ash layers were dated by Obradovich et al. (1982):

- ages at 2.22 ± 0.03 Ma (K/Ar, hornblende), 2.0 ± 0.16 Ma (fission-track, zircon), and 2.2 ± 0.2 Ma (fission track, glass) were obtained for ash a1;
- a questionable (probably too old) age at 1.99 ± 0.08 Ma (K/Ar, biotite) was obtained for ash a4.

Ash 1 was re-dated by the Isothermal Plateau Fission-Track (ITPFT) method, using its platy, hydrated glass shards (Westgate, 1989). Two age determinations were made, each based on a separate irradiation (Table 3). They are in close agreement and give a weighted mean age of 2.31 ± 0.34 Ma. This ITPFT age is slightly older than the K–Ar age on hornblende (2.22 ± 0.04 Ma) and the fission-track age on zircon (2.0 ± 0.16 Ma) and glass (2.2 ± 0.2 Ma) determined by Obradovich et al. (1982), but is highly consistent with the precise astronomical age of 2.31 Ma (insolation minimum

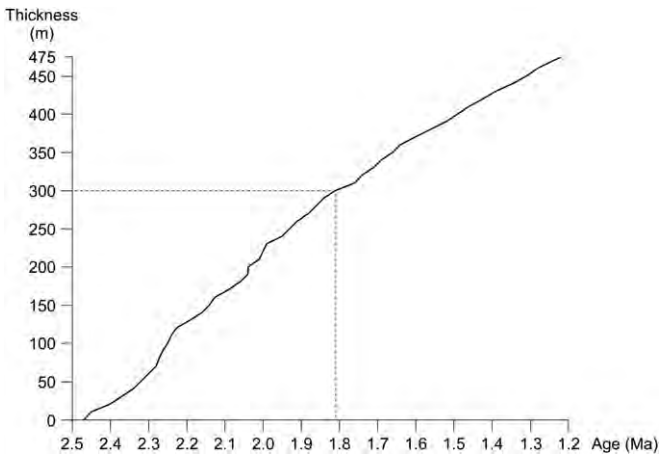

Fig. 6. Calculated sedimentation rate of the Crotone series.

Table 3
Glass fission-track age of ash a1 (UT 781).

Sample number	Date irradiated	Spontaneous track density 10^2 t/cm^2	Induced track density 10^5 t/cm^2	Track density on muscovite detector over dosimeter glass 10^5 t/cm^2	Etching conditions HF:temp:time %:°C:s	D_s/D_i	Age Ma
Ashai							
UT 781	13/6/1988	18.60 ± 2.44 (58)	1.75 ± 0.04 (1764)	7.42 ± 0.06 (14021)	26:25:80	0.99	2.37 ± 0.78
UT 781	19/11/1991	17.20 ± 1.17 (217)	1.40 ± 0.01 (9073)	6.25 ± 0.04 (27836)	26:25:90	0.98	2.30 ± 0.38
				Weighted mean age and error			2.31 ± 0.34
Moldavite tektite glass 19/11/1991		133 ± 5.23 (646)	1.73 ± 0.02 (5309)	6.17 ± 0.04 (27836)	26:22.5:135		14.26 ± 0.60

The age of Ash a1 (UT 781) was determined using the isothermal plateau fission-track method on glass shards in conjunction with the population-subtraction technique. Details are given in Westgate (1989), and Westgate et al. (2006). Correction for partial track fading was made using a thermal pretreatment of 150 °C for 30 days. Ages were calculated using the zeta approach and $\lambda_D = 1.551 \times 10^{-10}$ yr^{-1}. Zeta value is 301 ± 3 based on 6 irradiations at the McMaster Nuclear Reactor, Hamilton, Ontario, using the NIST SRM 612 glass dosimeter and the Moldavite tektite glass (Lhenice locality) with an $^{40}Ar/^{39}Ar$ age of 14.34 ± 0.08 Ma (Laurenzi et al., 2003, 2007). A sample of the Moldavite glass was irradiated in the same can as UT 781 and the fission-track counts gave an age very close to its accepted $^{40}Ar/^{39}Ar$ age of 14.34 ± 0.08 Ma. Error ($\pm 1\sigma$) on age estimate for UT 781 is calculated according to Bigazzi and Galbraith (1999). Area estimated using the point-counting method (Naeser et al., 1982) for UT 781 and an eyepiece reticule for the Moldavite glass. D_s = mean spontaneous track diameter, D_i = mean induced track diameter. Number of tracks counted is given in brackets. All samples etched to give D_i in range of 6–8 μm; equivalence of D_s and D_i under identical etch conditions indicates sample has been fully corrected for partial track fading.

supported by a coeval minimum in Riparian Trees), assigned to the level at which ash a1 occurs (Fig. 4H).

3. Additional results and comments

Because there is now complete agreement on the high-resolution Crotone series chronology, it is time to present some additional results and to offer some comments in order to achieve the knowledge of the entire series and to increase value of the very powerful Crotone sedimentary archive.

3.1. Tracking down the base of the series

Several scientific teams, including the authors, searched for studying sediments underlying the Semaforo section, where some additional sapropels have been detected. Unfortunately, the coastal road does not allow clear observations, and reliable stratigraphic correlations were unrealistic. However, it would be important to discover a continuous record to the earliest Northern Hemisphere glacial and the Gauss–Matuyama reversal. Performing a cored borehole at the base of the Semaforo section should therefore solve this problem.

3.2. Disruptions caused by precession in the vegetation climatic record

It has been pointed out that, for the Central and Eastern Mediterranean regions some vegetation reconstructions based on pollen records contradict the succession of the corresponding pollen floras inside a climatic cycle, especially displaying a glacial imprint

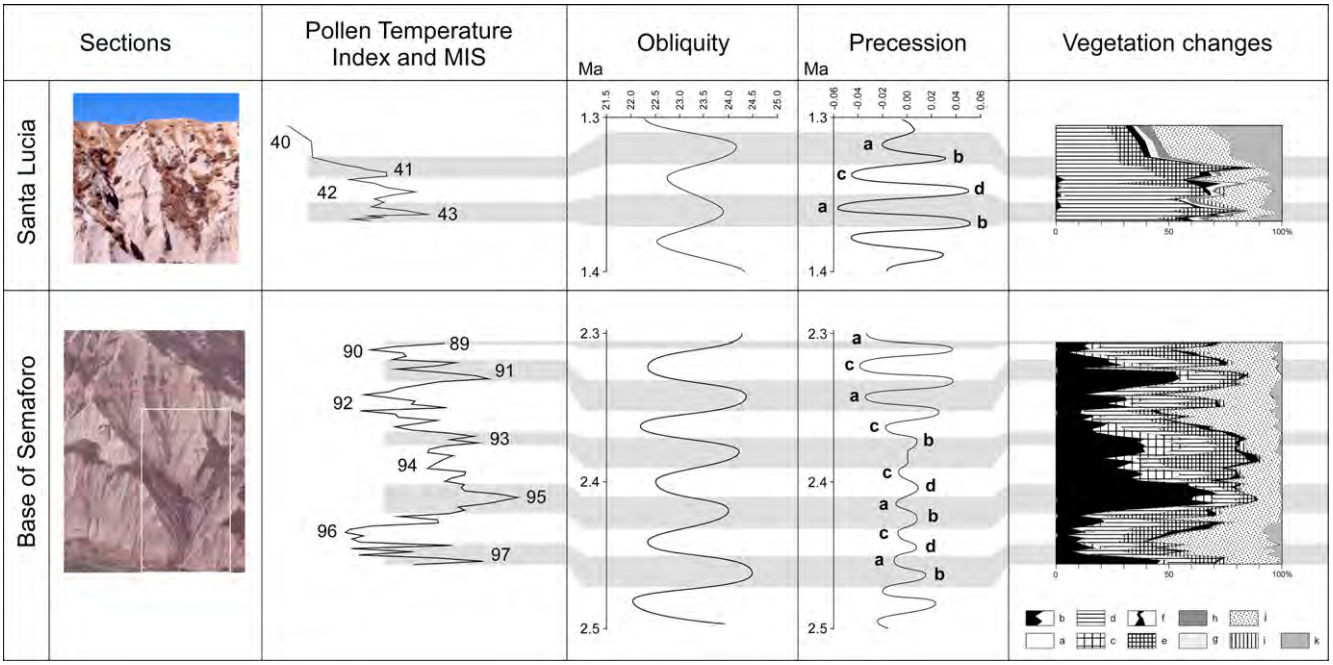

Fig. 7. Climate–vegetation detail on the base of the Semaforo (white rectangle on the photograph) and Santa Lucia sections. Light and dark bands emphasize the glacial–interglacial cycles on the Semaforo photograph. Interglacials are indicated by MIS numbers and grey bands, glacials are marked with white bands. They are respectively correlated to obliquity phases (Laskar et al., 2004). Vegetation changes are expressed by synthetic pollen diagrams (for details, see: Combourieu-Nebout, 1993; Joannin et al., 2007), the secondary fluctuations of which refer to precession variations (Laskar et al., 2004). (a) Tropical plants; (b) subtropical elements; (c) *Cathaya*; (d) warm-temperate elements; (e) mid-altitude trees; (f) high altitude trees; (g) elements without precise signification; (h) Cupressaceae; (i) Mediterranean xerophytes; (j) herbs; and (k) steppe elements. Relative influence of obliquity *vs.* precession: (a) obliquity maximum – precession minimum; (b) obliquity maximum – precession maximum; (c) obliquity minimum – precession minimum; and (d) obliquity minimum – precession maximum.

(steppe landscape) during an interglacial and vice versa (for a synthesis: Suc and Popescu, 2005). This contradiction has been successively clarified by Klotz et al. (2006) and Joannin et al. (2007) indicating that the precession forcing appeared as prominent in disrupting the control of obliquity. As this question was deciphered using pollen floras from the Crotone series, it is important to re-examine the concerned pollen records, i.e. from the base of Semaforo and Santa Lucia sections (Fig. 7).

In the lowermost 50 m of the Semaforo section, five interglacials and four glacials have been identified (Combourieu-Nebout, 1995), while two interglacials and two glacials were recorded at Santa Lucia (Joannin et al., 2007) (Figs. 4 and 7). They are directly related to obliquity maxima and minima, respectively. When a precession minimum (higher precipitation caused by intensified monsoon) occurred during a maximum of obliquity (interglacial) (situation "a" in Fig. 7), forest spread strengthened considerably. However, when a precession maximum (low precipitation in relation with decreased intensity of monsoon) occurred during a maximum of obliquity (interglacial) (situation "b" in Fig. 7), the expected interglacial forest development was reduced to the benefit of open vegetation. When a precession minimum occurred during an obliquity minimum (glacial) (situation "c" in Fig. 7), the forest recurred during a phase generally dominated by herbs. When a precession maximum occurred during an obliquity minimum (glacial) (situation "d" in Fig. 7), steppe conditions expressed its highest development.

Such a continuous competition between obliquity and precession signals left its complex imprint in the Central and Eastern Mediterranean pollen diagrams (see also Tzedakis, 2007) as illustrated in the lower part of both the base of the Semaforo and Santa Lucia sections (Fig. 7). The pollen diagram interpretations appears then more difficult by comparison to the Western Mediterranean archives where conditions are more contrasted probably in relation to the lower precession effect (interglacials are still humid and forested, glacials still dry and characterised by steppe; Suc and Popescu, 2005). At Santa Lucia glacials and interglacials are not as contrasted as at Semaforo because of the strong influence of almost coeval extensive precession minima (Joannin et al., 2007) (Fig. 7). Such an expected glacial–interglacial contrast is recovered in the uppermost part of the section because the precession influence decreased (weak minimum) (Fig. 7). These examples aim to partly illustrate how much the interaction between obliquity and precession is complex as shown by Becker et al. (2005).

3.3. Time-control during insolation maxima–precession minima

The large number of sapropels (some analysed in great detail: Suc et al., 1991; Van der Weijden, 1993; Negri et al., 2003; Cleaveland and Herbert, 2009) within the Crotone series and their thickness have largely contributed by making the series very attractive. A total organic carbon concentration between 0.2 and 0.8% has been found in these layers (Combourieu-Nebout, 1990; Suc et al., 1991), which is consistent with the values obtained by Howell et al. (1988, 1990) and Raffi and Thunell (1997). At the very most, they are only 'sapropelic' rocks from the carbon content viewpoint. Nevertheless, they are very obvious in the landscape and correspond to a significant change in sedimentation and environment as demonstrated by Hilgen (1991) and Lourens (1994). These layers have been particularly studied for their paleontological content (see for example: Landini and Menesini, 1978; Guerrera, 1981). The Crotone series anoxic layers display a hierarchy, pointed out by Combourieu-Nebout (1990) and Suc et al. (1991): the ultimate step (i.e. corresponding to maximum intensity in runoff and anoxia) corresponds to the sapropel itself, the intermediate step to the sapropelic clays, and the minor one is marked by an increase in amorphous organic matter and riparian tree pollen but lacking any lithological characteristics (Fig. 4).

In addition to the selected sapropel samples analysed for their pollen content (Combourieu-Nebout, 1987, 1990), a very high-resolution pollen analysis was performed on the thickest sapropel, i.e. sapropel 15 (c in the previous nomenclature; Fig. 8A). Here 41 samples were studied and compared to thirteen extra-sapropel samples, two of them being just at the limit of the sapropel (Fig. 8B; preliminary results in Suc et al., 1991). The pollen content of sapropel 15 is rather different from the underlying and overlying clays; this particularly results from the significant decrease in *Pinus* pollen grains within the sapropel despite some secondary fluctuations (Fig. 8B). This is a well-known phenomenon in sapropels which can be related to pollen transport when river input is important (Beaudouin et al., 2005, 2007): some other components such as the riparian trees are more abundant because of the increasing river input, which results in the relative decrease in *Pinus*. Total pollen concentration is significantly lower within the sapropel than in the over- or underlying clays and some sapropel samples close to its limits (Fig. 8B) which could be in relation with a sedimentation rate increase. Indeed, pollen concentration drops when repeated floods occur according to analyses of onshore and offshore samples deposited during the 1993–1994 (centennial) autumn–winter floods of the Rhône River (Suc, unpublished), observations in agreement

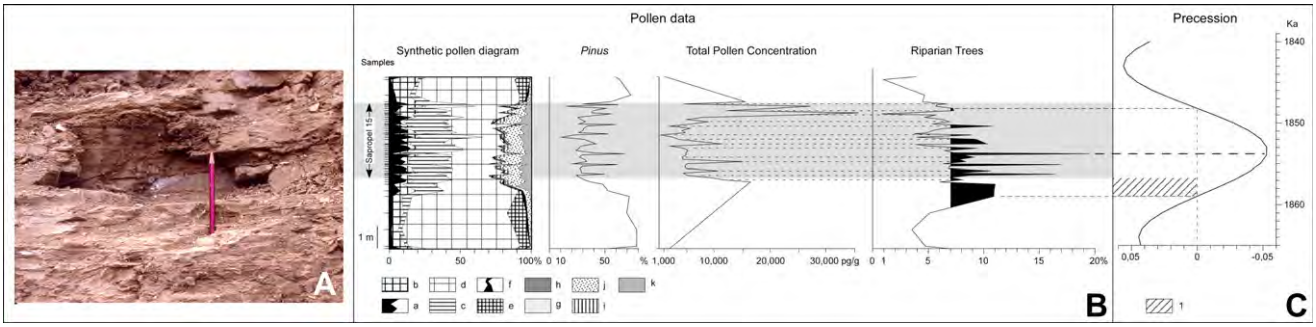

Fig. 8. High-resolution pollen study of sapropel 15 (i.e. c, Vrica B section). (A) Detail view of sapropel 15. (B) Synthetic pollen diagram and some other pollen indicators: percentages in *Pinus*; total pollen concentration; riparian trees as listed in Fig. 4I the maxima of which exceeding 7% are black-coloured. The dotted lines point out the correlation between maxima of riparian trees and the total pollen concentration. The sapropel extent is indicated by a grey band. Legend of the synthetic pollen diagram: (a) subtropical elements; (b) *Cathaya*; (c) warm-temperate elements; (d) *Pinus* and indeterminabe Pinaceae; (e) mid-altitude trees; (f) high altitude trees; (g) elements without precise signification; h, Cupressaceae; (i) Mediterranean xerophytes; (j) herbs; (k) steppe elements. (C) Precession curve for the time-interval 1.865–1.839 Ma (Laskar et al., 2004). The thick dotted line shows the correlation of maximum in riparian trees (i.e. maximum of runoff) with minimum of precession; the thin dotted lines indicate the first and last maxima in riparian trees (>7%) correlated with the reversal of precession from positive to negative values and vice versa. The grey band illustrates the proposed correlation with sapropel 15:1, delay in response of the sapropel formation to runoff increase.

with a long record from the Grand Rhône prodeltaic muds covering the last 60 years (Beaudouin et al., 2005). This is caused by dilution of pollen grains within increasing terrigenous material.

The riparian trees are more represented within the sapropel (especially within its lower two thirds) than in the clays. Their decrease in the upper last third of the sapropel may indicate rarefying floods and hence diminishing river input that is also attested by more elevated total pollen concentration (Fig. 8B).

These observations raise new questions:

- is the thickness of a sapropel proportional to duration and/or intensity of anoxia and, hence, of runoff?
- how long does a sapropel represent in time within the precession cycle: ca. 11 kyr, i.e. the half of the cycle or only the peak of the precession minimum?

Sapropel 15 (3.38 m in thickness) correlates with insolation maximum i-180 (Fig. 4A, I, H). Peak i-180 is no longer than the other insolation maxima resulting in a well-expressed sapropel, but it is one of the most elevated maxima (with i-216 and i-130) during the time-interval considered between 2.5 and 1.2 Ma, thus coinciding with a eccentricity maximum (Fig. 4H). In addition, peak i-180 is almost synchronous to an obliquity maximum (i.e. interglacial conditions), that slightly differs from i-216 and i-130 peaks (sapropels 5 and 29, respectively; Fig. 4A and I). The latter occurred during a little less intense eccentricity maximum (Fig. 4H). Some equivalent intense insolation maxima (e.g. i-170 and i-140) also occurred during less prominent eccentricity maxima (Fig. 4H). As a consequence, the authors consider that runoff intensity represents the main forcing parameter for sapropel development. Insolation maximum i-180 probably corresponded to the best conditions for optimal rainfall over the nearby Sila Massif. Indeed, the percentage of plants requiring high humidity in sapropel 15 is the highest (55–77%) among all sapropels archived in the Crotone series. The percentage of riparian trees is also among the largest recorded in the Crotone series except for the Santa Lucia section which probably relates to the progressive shallowing conditions in the basin (as uplift caused the sediments to be close to exposure), the frequency in riparian trees of which (16–20%; Fig. 4I) is very similar to those recorded at the mouth of the Rhône River today (Beaudouin et al., 2005).

The insolation maximum i-180 is one of the shortest recorded in the Crotone series, while the synchronous precession minimum corresponds to a decreasing phase (i.e. negative values) shorter (5.1 ky) than the following rising phase (5.6 ky) (Fig. 8C). Maxima in riparian trees (>7%) display a progressive-regressive distribution which looks like the precession fluctuation, and they clearly appeared significantly before the sapropel deposition. This succession (runoff evidence followed by sapropel deposition) recalls the above-mentioned hierarchy where sapropel is the ultimate step of the record of anoxic conditions. Accordingly, considering the high sensitivity of the riparian tree frequency as Runoff Index, its earliest peak (>7%) is correlated to the first precession negative values, the latest one with the return to positive precession values and the riparian tree highest maximum with the precession minimum (Fig. 8B and C). In this way, the uppermost sapropel sediments correspond to the first positive precession values and to a secondary riparian tree maximum (Fig. 8B and C). Sapropel deposition appears then shifted with respect to the positive–negative passage in precession values and reciprocally, the delay being more accentuated in the progression towards the precession minimum (2.3 ky) than towards the next precession maximum (0.8 ky) (Fig. 8C). The resulting sapropel 15 duration corresponds to 9.18 ky (Fig. 8C), a value somewhat different from that obtained in using annual lamina couplets (6.76 ky; Negri et al., 2003). Sapropels cored in hole h3 display a weak laminated feature. Thus, as a well-marked lamination seems exaggerated by sapropel exposition, the sapropel 15 duration proposed by Negri et al. (2003) must be regarded with caution.

Negri et al. (2003) proposed three reconstructed environmental phases for sapropel 15 using nannoplankton and foraminifers, summarized as follows:

- lowermost 118 cm, cold superficial water and strongly dysoxic sea bottom;
- median 98 cm, stratified superficial water, high seasonality;
- uppermost 122 cm, slight sea-bottom reoxygenation, warm superficial water, upwelling, CO_2 rich water.

After comparison with our riparian tree curve, these subdivisions correspond to optimal, reduced, and rarefied river discharges, respectively (Fig. 8B).

Practically, almost all riparian tree maxima (9 on a total of 13 recorded within the sapropel 15) are correlated with total pollen concentration minima (dotted lines, Fig. 8B). They correspond to the river flood signature, as shown for the present-day Rhône system (Beaudouin et al., 2005), and might correspond to the well-known millennial rhythm of the greatest river floods. This reliable approach suggests that a sapropel represents slightly less than half of an insolation cycle. Nevertheless, it appears unsuitable to relate sapropel thickness and its duration because the former was more linked to the quantity of the transported terrigenous material. Comparison between sapropels 15 and 29, respectively, corresponding to insolation maxima i-180 and i-130, demonstrates that they correspond to almost similar astronomical conditions (insolation intensity, location within obliquity and eccentricity cycles) while their thickness differs by a ratio of 4/1.

4. Conclusion

The new Crotone series data indicate:

- a strengthened stratigraphic correlation between the Semaforo and Vrica areas based on field surveys, a cored borehole, and ash mineralogy and geochemistry;
- a widely accepted accurate chronology with respect to insolation parameters (eccentricity, obliquity, precession) resulting from complementary reliable biostratigraphy, magnetostratigraphy and cyclostratigraphy.

Its chronological extent runs from 2.47 to 1.21 Ma, including a continuous reference to glacial–interglacial and insolation cycles, respectively. Such an accurate study probably results from the strong desire to define the Pliocene–Pleistocene boundary in the Vrica section and from the international debate which followed this decision. However, a better international coordinated research would have sometimes benefited from more quietness during such intensive investigations.

The Crotone series is certainly the global exposed reference for the earliest glacial–interglacial cycles of the Northern Hemisphere. New aspects are very promising for future researches, such as (1) the partly deciphered complex interaction between obliquity and precession and their respective impact on vegetation changes in the Central and Eastern Mediterranean regions, and (2) extending the alkenone study to the entire series. Finally, new prospects should follow from pollen investigations of present-day sediments which would provide a more complete understanding of anoxic deposits, the intensity and duration of which being narrowly linked to respective influence of precession, eccentricity and obliquity, as confirmed at Crotone.

Acknowledgements

TOTAL, ELF, and CNRS/INSU provided the financial support for performing the cored hole h3. Paleomagnetic measurements on borehole h3 were realized at the Geosciences Institute of the Montpellier University. Jacques Cravatte and Pascal Guenet contributed very actively to the coring process. Claude Poumot provided a highly appreciated support. Professor Enrico Franza provided facilities for our successive stays at Crotone. Dr. Salvatore Via, the owner of the land where the borehole h3 was cored, is acknowledged for his kind authorization. Professor Philip Gibbard friendly reviewed the manuscript and edited the English. We especially thank the reviewers, S.A.G. Leroy and F.J. Hilgen who, by their comments, helped us to improve the manuscript and to develop a fruitful discussion. N. Catto, Editor-in-Chief of Quaternary International, is also acknowledged for his help and consideration. Finally, we want to thank M.B. Cita and B. Pillans who invited us to perform this synthesis on the Crotone series.

References

Aguirre, E., Pasini, G., 1985. The Pliocene–Pleistocene boundary. Episodes 8, 116–120.

Argani, A., Savelli, C., 1999. Cenozoic volcanism and tectonics in the southern Tyrrhenian Sea: space–time distribution and geodynamic significance. Geodynamics 27, 409–432.

Barbieri, M., Di Girolamo, P., Locardi, E., Lombardi, G., Stanzione, D., 1979. Petrology of the calc-alkaline volcanics of the Parete-2 well (Campania, Italy). Periodico di Mineralogia 48, 53–74.

Barone, A., Fabri, A., Rossi, S., Sartori, R., 1982. Geological structure and evolution of the marine areas adjacent to the Calabria Arc. Earth Evolution Sciences 3, 207–221.

Beaudouin, C., Suc, J.-P., Cambon, G., Touzani, A., Giresse, P., Pont, D., Aloïsi, J.-C., Marsset, T., Cochonat, P., Duzer, D., Ferrier, J., 2005. Present-day rhythmic deposition in the Grand Rhône prodelta (NW Mediterranean) according to high-resolution pollen analyses. Journal of Coastal Research 21 (2), 292–306.

Beaudouin, C., Suc, J.-P., Escarguel, G., Arnaud, M., Charmasson, S., 2007. The significance of pollen signal in present-day marine terrigenous sediments: the example of the Gulf of Lions (western Mediterranean Sea). Geobios 40, 159–172.

Beccaluva, L., Bonatti, E., Dupuy, C., Ferrara, G., Innocenti, F., Lucchini, F., Macera, P., Petrini, R., Rossi, P.L., Serri, G., Seyler, M., Siena, F., 1990. Geochemistry and mineralogy of the volcanic rocks from ODP sites 650, 651, 655, and 654 in the Tyrrhenian Sea. In: Kastens, K.A., Mascle, J., et al. (Eds.), Leg 107. Proceedings of the Ocean Drilling Program, Scientific Results 107, 49–74.

Becker, J., Lourens, L.J., Hilgen, F.J., van der Laan, E., Kouwenhoven, T.J., Reichart, G.-J., 2005. Late Pliocene climate variability on Milankovitch to millennial time scales: A high-resolution study of MIS100 from the Mediterranean. Palaeogeography, Palaeoclimatology, Palaeoecology 228, 338–360.

Bigazzi, G., Galbraith, R.F., 1999. Point-counting technique for fission-track dating of tephra glass shards, and its relative standard error. Quaternary Research 51, 67–73.

Cadoux, A., Pinti, D.L., Aznar, C., Chiesa, S., Gillot, P.Y., 2005. New chronological and geochemical constraints on the genesis and evolution of Ponza and Palmarola volcanic islands (Tyrrhenian Sea, Italy). Lithos 81, 121–151.

Cati, F., Borsetti, A.M., 1981. Calcareous nannoplankton biostratigraphy of the Vrica Section (Calabria, Southern Italy). Giornale di Geologia 43, 365–384.

Ciaranfi, N., D'Alessandro, A., 2005. Overview of the Montalbano Jonico area and section: a proposal for a boundary stratotype for the lower-middle Pleistocene, Southern Italy Foredeep. Quaternary International 131, 5–10.

Cleaveland, L.C., Herbert, T.D., 2009. Preservation of the alkenone paleotemperature proxy in uplifted marine sequences: A test from the Vrica outcrop, Crotone, Italy. Geology 37 (2), 179–182.

Colalongo, M.L., Pasini, G., Sartoni, S., 1981. Remarks on the Neogene/Quaternary boundary and the Vrica section (Calabria, Italy). Bollettino della Società Paleontologica Italiana 20, 99–120.

Combourieu-Nebout, N., 1987. Les premiers cycles glaciaire-interglaciaire en région méditerranéenne d'après l'analyse palynologique de la série plio-pléistocène de Crotone (Italie méridionale). PhD thesis, University Montpellier 2, 161 pp.

Combourieu-Nebout, N., 1990. Les cycles glaciaire-interglaciaire en région méditerranéenne de 2,4 à 1,1 Ma: Analyse pollinique de la série de Crotone (Italie méridionale). Paléobiologie Continentale 17, 35–59.

Combourieu-Nebout, N., 1993. Vegetation response to upper Pliocene glacial/interglacial cyclicity in the central Mediterranean. Quaternary Research 40, 228–236.

Combourieu-Nebout, N., 1995. Réponse de la végétation de l'Italie méridionale au seuil climatique de la fin du Pliocène d'après l'analyse pollinique haute résolution de la section de Semaforo (2,46 à 2,1 Ma). Comptes-Rendus de l'Académie des Sciences de Paris Ser. IIa 321, 659–665.

Combourieu-Nebout, N., Fauquette, S., Quézel, P., 2000. What was the late Pliocene Mediterranean climate like: a preliminary quantification from vegetation. Bulletin de la Société géologique de France 171 (2), 271–277.

Combourieu-Nebout, N., Sémah, F., Djubiantono, T., 1990. La limite Pliocène–Pléistocène: précisions magnétostratigraphiques et climatiques par l'étude sériée de la coupe-type de Vrica (Crotone, Italie). Comptes-Rendus de l'Académie des Sciences de Paris Ser. II 311, 851–857.

Combourieu-Nebout, N., Vergnaud Grazzini, C., 1991. Late Pliocene Northern Hemisphere glaciations: the continental and marine responses in the central Mediterranean. Quaternary Science Reviews 10, 319–334.

Cowie, J.W., Ziegler, W., Boucot, A.J., Bassett, M.G., Remane, J., 1986. Guidelines and statutes of the International Commission on Stratigraphy (ICS). Courier Forschungsinstitut Senckenberg 100, 53–107.

Di Girolamo, P., Franciosi, L., Melluso, L., Morra, V., 1997. The calcalkaline rocks of the Campanian plain: new mineral chemical data and possible links with the acidic rocks of the Pontine islands. Periodico di Mineralogia 65, 305–316.

D'Onofrio, S., 1981. I Foraminiferi bentonici della Sezione Vrica (Calabria, Italia). Giornale di Geologia 43, 327–364.

Gautier, F., 1990. Magnétostratigraphie du sondage Vrica S3 et du sommet de la coupe de Semaforo (Série plio-pléistocène de Crotone, Italie). Master Paleontology, University Montpellier 2, 36 pp.

Guerrera, F., 1981. Caratteristiche sedimentologiche e micropaleontologiche dei depositi tripolacei plio-quaternari del bacino crotonese (Calabria). Acta Naturalia de l'Ateneo Parmense 17, 113–138.

Guerrera, F., Veneri, F., 1989. Evidenze di attività vulcanica nei sedimenti neogenici e pleistocenici dell'Appennino: stato delle conoscenze. Bollettino della Società Geologica Italiana 108, 121–160.

Head, M.J., Gibbard, P., Salvador, A., 2008. The Quaternary: its character and definition. Episodes 31 (2), 234–238.

Hilgen, F.J., 1990. Closing the gap in the Plio–Pleistocene boundary stratotype sequence of Crotone (southern Italy). Newsletters of Stratigraphy 22 (1), 43–51.

Hilgen, F.J., 1991. Astronomical calibration of Gauss to Matuyama sapropels in the Mediterranean and implication for the geomagnetic Polarity Time Scale. Earth and Planetary Science Letters 104, 226–244.

Howell, M.W., Rio, D., Thunell, R.C., 1990. Laminated sediments from the Vrica section (Calabria, S. Italy): evidence for Plio-Pleistocene climatic change in the Mediterranean region. Palaeogeography, Palaeoclimatology, Palaeoecology 78, 195–216.

Howell, M.W., Thunell, R.C., Tappa, E., Rio, D., Sprovieri, R., 1988. Late Neogene laminated and opal-rich facies from the Mediterranean region: geochemical evidence for mechanisms of formation. Palaeogeography, Palaeoclimatology, Palaeoecology 64, 265–286.

Joannin, S., Quillévéré, F., Suc, J.-P., Lécuyer, C., Martineau, F., 2007. Early Pleistocene climate changes in the central Mediterranean region as inferred from integrated pollen and planktonic foraminiferal stable isotope analyses. Quaternary Research 67, 364–374.

Klotz, S., Fauquette, S., Combourieu-Nebout, N., Uhl, D., Suc, J.-P., Mosbrugger, V., 2006. Seasonality intensification and long-term winter cooling as a part of the Late Pliocene climate development. Earth and Planetary Science Letters 241, 174–187.

Landini, W., Menesini, E., 1978. L'Ittiofauna Plio-Pleistocenica della sezione della Vrica (Crotone-Calabria). Bollettino della Società Paleontologica Italiana 17, 143–175.

Laskar, J., Robutel, P., Joutel, F., Gastineau, M., Correia, A., Levrand, B., 2004. A long-term numerical solution for the insolation quantities of the Earth. Astronomy and Astromhysics 428, 261–285.

Laurenzi, M.A., Bigazzi, G., Balestrieri, M.L., Bouska, V., 2003. $^{40}Ar/^{39}Ar$ laser probe dating of the Central European tektite-producing impact event. Meteoritics and Planetary Science 38, 887–893.

Laurenzi, M.A., Balestrieri, M.L., Bigazzi, G., Hadler Neto, J.C., Iunes, P.J., Norelli, P., Oddone, M., Osorio Araya, A.M., Viramonte, J.G., 2007. New constraints on ages of glasses proposed as reference materials for fission-track dating. Geostandards and Geoanalytical Research 31, 105–124.

Leake, B.E., et al., 1997. Nomenclature of amphiboles report of the subcommittee on amphiboles of the international mineralogical association, commission on new minerals and mineral names. The Canadian Mineralogist 35, 219–246.

Letterier, J., Maury, R.C., Thonon, P., Girard, D., Marchal, M., 1982. Clinopyroxene composition as a method of identification of magmatic affinities of paleovolcanic series. Earth and Planetary Science letters 59, 139–154.

Lourens, L.J., 1994. Astronomical Forcing of Mediterranean Climate During The last 5.3 Million Years. PhD thesis, Utrecht University, 247 pp.

Lourens, L.J., Hilgen, F.J., Laskar, J., Shackleton, N.J., Wilson, D., 2004. The Neogene period. In: Gradstein, F.M., Ogg, J.G., Smith, A.G. (Eds.), A Geological Time Scale 2004. Cambridge University Press, Cambridge, pp. 409–440.

Lourens, L.J., Hilgen, F.J., Raffi, I., Vergnaud-Grazzini, C., 1996. Early Pleistocene chronology of the Vrica section (Calabria, Italy). Paleoceanography 11, 797–812.

Lourens, L.J., Hilgen, F.J., Raffi, I., 1998. Base of Large *Gephyrocapsa* and astronomical calibration of Early Pleistocene sapropels in Site 967 and Hole 969D: solving the chronology of the Vrica section (Calabria, Italy). In: Robertson, A.H.F., Emeis, K.-C., Richter, C., Camerlenghi, A. (Eds.), Leg 160. Proceedings of the Ocean Drilling Program, Scientific Results 160, 191–197.

Morimoto, N., subcommittee members, 1988. Nomenclature of pyroxenes. American Mineralogist 73, 1123–1133.

Naeser, N.D., Westgate, J.A., Hughes, O.L., Péwé, T.L., 1982. Fission-track ages of late Cenozoic distal tephra beds in the Yukon and Alaska. Canadian Journal of Earth Sciences 19, 2164–2178.

Nakagawa, H., 1981. Neogene/Quaternary boundary and correlation of Vrica Section. In: Sastry, M.V.A., et al. (Eds.), Field Conference, Neogene–Quaternary Boundary, India 1979: Proceedings. Geological Survey of India, Calcutta, pp. 107–111.

Nakagawa, H., Niitsuma, N., Takayama, T., Matoba, Y., Oda, M., Tokunaga, S., Kitazato, H., Sakai, T., Koizumi, I., 1997. The magnetostratigraphy of the Vrica section, Italy, and its correlation with the Plio–Pleistocene of the Boso Peninsula, Japan. In: Van Couvering, J.A. (Ed.), The Pleistocene Boundary and the Beginning of the Quaternary. Cambridge University Press, pp. 46–56.

Negri, A., Morigi, C., Giunta, S., 2003. Are productivity and stratification important to sapropel deposition? Microfossil evidence from late Pliocene insolation cycle 180 at Vrica, Calabria. Palaeogeography, Palaeoclimatology, Palaeoecology 190, 243–255.

Obradovich, J.D., Naeser, C.W., Izett, G.A., Pasini, G., Bigazzi, G., 1982. Age constraints of the proposed Plio–Pleistocene boundary stratotype at Vrica, Italy. Nature 298, 55–59.

Partridge, T.C., 1997. Reassessment of the position of the Plio–Pleistocene boundary: is there a case for lowering it to the Gauss–Matuyama palaeomagnetic reversal? Quaternary International 40, 5–10.

Pasini, G., Colalongo, M.L., 1997. The Pliocene–Pleistocene boundary-stratotype at Vrica, Italy. In: Van Couvering, J.A. (Ed.), The Pleistocene Boundary and the Beginning of the Quaternary. Cambridge University Press, pp. 15–45.

Peccerillo, A., 2005. Plio-Quaternary Volcanism in Italy: Petrology, Geochemistry, Geodynamics. Springer-Verlag, Berlin, Heidelberg.

Prosser, G., Bentivenga, M., Laurenzi, M.A., Caggianelli, A., Dellino, P., Doronzo, D., 2008. Late Pliocene volcaniclastic products from Southern Apennines: distal witness of early explosive volcanism in the central Tyrrhenian Sea. Geological Magazine 145, 521–536.

Raffi, I., Thunell, R., 1997. Comparison of the laminated units at vrica and deep-sea sapropels from the eastern Mediterranean. In: Van Couvering, J.A. (Ed.), The Pleistocene Boundary and the Beginning of the Quaternary. Cambridge University Press, pp. 57–62.

Rio, D., Raffi, I., Backman, J., 1997. Calcareous nannofossil biochronology and the Pliocene–Pleistocene boundary. In: Van Couvering, J.A. (Ed.), The Pleistocene Boundary and the Beginning of the Quaternary. Cambridge University Press, pp. 63–78.

Savelli, C., 1988. Late Oligocene to Recent episodes of magmatism in and around the Tyrrhenian Sea: implications for the processes of opening in a young interarc basin of intra-orogenic (Mediterranean) type. Tectonophysics 146, 163–181.

Selli, R., Accorsi, C.A., Bandini Mazzanti, M., Bertolani Marchetti, D., Bigazzi, G., Bonadonna, F.P., Borsetti, A.M., Cati, F., Colalongo, M.L., D'Onofrio, S., Landini, W., Menesini, E., Mezzetti, R., Pasini, G., Savelli, C., Tampieri, R., 1977. The Vrica section (Calabria, Italy). A potential Neogene/Quaternary boundary stratotype. Giornale di Geologia 42, 181–201.

Spaak, P., 1983. Accuracy in correlation and ecological aspects of the planktonic foraminiferal zonation of the Mediterranean Pliocene. Utrecht Micropaleontological Bulletins 28, 5–160.

Spadea, P., 1986. Volcanogenic deposits in Fossa Bradanica (Southern Italy): records of calcalkaline and alkaline volcanism during the Pliocene and Pleistocene in the Mediterranean. Neues Jahrbuch für Mineralogie Abhandlungen 153 (2), 217.

Suc, J.-P., Popescu, S.-M., 2005. Pollen records and climatic cycles in the North Mediterranean region since 2.7 Ma. In: Head, M.J., Gibbard, P.L. (Eds.), Early–Middle Pleistocene Transitions: the Land–Ocean Evidence. Geological Society of London, Special Publication, vol. 247, pp. 147–158.

Suc, J.-P., Zagwijn, W.H., 1983. Plio–Pleistocene correlations between the northwestern Mediterranean region and northwestern Europe according to recent biostratigraphic and palaeoclimatic data. Boreas 12, 153–166.

Suc, J.-P., Bertini, A., Leroy, S.A.G., Suballyova, D., 1997. Towards the lowering of the Pliocene/Pleistocene boundary to the Gauss–Matuyama reversal. Quaternary International 40, 37–42.

Suc, J.-P., Combourieu-Nebout, N., Robert, C., Poumot, C., Turon, J.-L., Irr, F., 1991. Changements dans la sédimentation argileuse au Néogène supérieur en Méditerranée centrale: les Tripoli messiniens de Capodarso (Sicile) et les laminites plio-pléistocènes de Crotone (Calabre). Palynosciences 1, 89–111.

Tauxe, L., Opdyke, N.D., Pasini, G., Elmi, C., 1983. Age of the Plio–Pleistocene boundary in the Vrica section, southern Italy. Nature 304, 125–129.

Tzedakis, P.C., 2007. Seven ambiguities in the Mediterranean palaeoenvironmental narrative. Quaternary Science Reviews 26, 2042–2066.

Van der Weijden, C.H., 1993. Geochemical signatures preserved in sediments of the Semaforo and Vrica sections (Calabria, Italy) and their relations with variations of the sedimentary regime. Palaeogeography, Palaeoclimatology, Palaeoecology 103, 203–221.

Westgate, J.A., 1989. Isothermal plateau fission track ages of hydrated glass shards from silicic tephra beds. Earth and Planetary Sciences Letters 95, 226–234.

Westgate, J.A., Naeser, N.D., Alloway, B.V., 2006. Fission-track dating. In: Elias, S.A. (Ed.), Encylopedia of Quaternary Science. Elsevier Publishers, Amsterdam, pp. 651–672.

Zagwijn, W.H., 1974. The Plio–Pleistocene boundary in western and southern Europe. Boreas 3, 75–97.

Zecchin, M., Mellere, D., Roda, C., 2006. Sequence stratigraphy and architectural variability in growth fault-bounded basin fills: a review of Plio-Pleistocene strata units of the Crotone Basin, southern Italy. Journal of the Geological Society, London 163, 471–486.

Zijderveld, J.D.A., Hilgen, F.J., Langereis, C.G., Verhallen, P.J.J.M., Zachariasse, W.J., 1991. Integrated magnetostratigraphy and biostratigraphy of the upper Pliocene–lower Pleistocene from the Monte Singa and Crotone areas in Calabria, Italy. Earth and Planetary Science Letters 107, 697–714.